Temperature-Dependent Kinetics Study of the Gas-Phase Reactions of OH with *n*- and *i*-Propyl Bromide

Mikhail G. Bryukov, Rebecca G. Vidrine, and Barry Dellinger*

Department of Chemistry, Louisiana State University, Baton Rouge, Louisiana 70803

Received: April 5, 2007; In Final Form: May 16, 2007

An experimental, temperature-dependent kinetics study of the gas-phase reactions of hydroxyl radical with *n*-propyl bromide, OH + *n*-C_3H_7Br → products (reaction 1), and *i*-propyl bromide, OH + *i*-C_3H_7Br → products (reaction 2), has been performed over wide ranges of temperatures 297−725 and 297−715 K, respectively, and at pressures between 6.67 and 26.76 kPa by a pulsed laser photolysis/pulsed laser-induced fluorescence technique. Data sets of absolute bimolecular rate coefficients obtained in this study for reactions 1 and 2 demonstrate no correlation with pressure and exhibit positive temperature dependencies that can be represented with modified three-parameter Arrhenius expressions within their corresponding experimental temperature ranges: $k_1(T) = (1.32 \times 10^{-17})T^{1.95} \exp(+25/T)$ cm^3 molecule^{-1} s^{-1} for reaction 1 and $k_2(T) = (1.56 \times 10^{-24})T^{4.18}\exp(+922/T)$ cm^3 molecule^{-1} s^{-1} for reaction 2. The present results, which extend the current kinetics data base of reactions 1 and 2 to high temperatures, are compared with those from previous works. On the basis of the present data and available data from previous studies, the following bimolecular rate coefficient temperature dependencies can be recommended for the purpose of kinetic modeling: $k_1(T) = (1.89 \times 10^{-19})T^{2.54}\exp(+301/T)$ cm^3 molecule^{-1} s^{-1} for reaction 1 in a temperature range 210−725 K, and $k_2(T) = (2.83 \times 10^{-21})T^{3.1}\exp(+521/T)$ cm^3 molecule^{-1} s^{-1} and $k_2(T) = (4.54 \times 10^{-24})T^{4.03}\exp(+860/T)$ cm^3 molecule^{-1} s^{-1} for reaction 2 in temperature ranges 210−480 and 297−715 K, respectively.

I. Introduction

Reactions of hydrogen-atom abstraction by hydroxyl radicals are important components of complex processes such as the chemistry of the Earth's atmosphere, combustion, and incineration of industrial wastes. Reaction kinetic modeling of these processes is useful for understanding their mechanisms, which can be used as a tool of prediction and control of pollutant emissions. Numerical simulations of the complicated chemistry of these phenomena require a large data base of accurately determined reaction rate coefficients spanning a wide range of temperatures and pressures. In this article, we report the results of our experimental, temperature-dependent kinetics investigation of the reactions of the hydroxyl radical with *n*-propyl bromide ($CH_3CH_2CH_2Br$) and *i*-propyl bromide ($CH_3CHBrCH_3$) over wide temperature ranges:

$$OH + n\text{-}C_3H_7Br \rightarrow \text{products} \quad (1)$$

$$OH + i\text{-}C_3H_7Br \rightarrow \text{products} \quad (2)$$

n-Propyl bromide (1-bromopropane) is a chemical widely used as an industrial solvent for spray adhesives, fats, waxes, and resins and as a synthetic intermediate. Adoption of *n*-propyl bromide as a replacement for some high-end halogenated ozone-depleting solvents will likely increase its worldwide annual consumption, recently estimated between 5000 and 10 000 metric tons.[1] *i*-Propyl bromide (2-bromopropane) is not produced deliberately for commercial purposes in large quantities, but it is present in commercially produced *n*-propyl bromide in concentrations of approximately 0.1−0.2% as an inevitable contaminant in *n*-C_3H_7Br synthesis. Thus, significant amounts of *n*- and *i*-propyl bromide can be subjected to thermal degradation in hazardous and municipal waste incinerators or accidental fires.

As with any volatile organic compound, molecules of these bromopropanes can be released to the atmosphere through evaporation at the Earth's surface and reach the stratosphere, where they can catalytically deplete ozone. The atmospheric and combustion chemistry of these bromopropanes appears to be very unusual compared to typical organic compounds and relatively complex because of the presence of bromine. This has stimulated the study of the physicochemical properties of *n*- and *i*-propyl bromide to understand their impact on the environment.

To our knowledge, there have been six[2−7] and four studies[2,3,5,7] on the kinetics of reactions 1 and 2, respectively, at the low-temperature range. The experiments on the kinetics study of reactions 1 and 2 performed in previous works cover a temperature range from 210 to 480 K, which is relevant to atmospheric chemistry. It was well-established that reactions 1 and 2 are primary loss processes for *n*- and *i*-propyl bromide in the atmosphere.[2−7] Reactions 1 and 2 proceed through exothermic H-atom abstraction channels, generating H_2O and the corresponding brominated propyl radicals, while abstractions of the Br atom from *n*- and *i*-C_3H_7Br are highly endothermic processes that can be neglected.[5,6,8−13]

Presently, it is difficult to evaluate the role of OH reactions with brominated hydrocarbons (BHCs) in the chemistry of combustion and thermal degradation processes, because there is a lack of fundamental information on the rate coefficients of a large number of elementary processes involving BHC molecules and radicals. Nevertheless, we can assume that the

* To whom correspondence should be addressed: e-mail BarryD@LSU.edu.

10.1021/jp072693c CCC: $37.00
Published on Web 06/27/2007

reaction of H-atom abstraction by the OH radical from a BHC is one of the primary processes of BHC consumption, which should directly compete with BHC unimolecular decomposition and the H + BHC reaction.

The present work represents the first experimental kinetics study of reactions 1 and 2 carried out at high temperatures extending from 297 K (to compare with the results of the earlier low-temperature studies) to 725 and 715 K, respectively.

II. Experimental Section

II.A. Experimental Technique. Absolute rate coefficients for the reactions of hydroxyl radicals with *n*- and *i*-propyl bromide were measured by the pulsed laser photolysis/pulsed laser-induced fluorescence (PLP/PLIF) technique. All experiments were carried out in a slow-flow, heatable quartz reactor (reaction cell) under pseudo-first-order conditions with a large excess of molecular substrate (*n*- or *i*-C_3H_7Br). A detailed description of the experimental setup, data acquisition methodology, and data processing has been given in our previous articles.[14,15] Therefore, only the details necessary to understand the present measurements are considered here.

Hydroxyl radicals were generated by pulsed laser photolysis (the repetition frequency was 10 Hz) in the reaction cell via two different ways. In some experiments, hydroxyl radicals were formed by 193-nm (ArF excimer) laser photolysis of N_2O to $O(^1D)$ and N_2, followed by the subsequent rapid reaction of $O(^1D)$ with H_2O:[16,17]

$$N_2O + h\nu(193\ \text{nm}) \rightarrow N_2 + O(^1D) \quad (3)$$

$$O(^1D) + H_2O \rightarrow 2OH \quad (4)$$

When *n*- or *i*-C_3H_7Br was present in the reaction mixture, OH could potentially be produced via reactions of $O(^1D)$ with one of these species that can occur simultaneously with reaction 4. In other experiments, we produced hydroxyl radicals by 248-nm (KrF excimer) laser photolysis dissociation of HNO_3:[18]

$$HNO_3 + h\nu(248\ \text{nm}) \rightarrow OH + NO_2 \quad (5)$$

to verify that the results were independent of the method of OH generation and laser photolysis wavelength.

After the excimer laser pulse, a second pulse at approximately 282 nm from a Nd:YAG-pumped, frequency-doubled, tunable pulsed dye laser induced excitation of the hydroxyl radicals via the $A^2\Sigma^+ - X^2\Pi$ (1−0) transition. Hydroxyl radicals were observed via fluorescence from the (1−1) and (0−0) bands at 308−316 nm.[19,20] The fluorescent radiation emitted perpendicular to the plane defined by the two laser beams was detected with a photomultiplier tube, by use of appropriate filters (308 nm peak transmission) to minimize scattered light. The signal from the photomultiplier was amplified and then recorded by a digital oscilloscope. The oscilloscope obtained the integrated voltage averaged for a desired number of the accumulated signals (typically 50−150) at a given time delay between the excimer laser and Nd:YAG laser pulses. This time delay was varied to record kinetic information by use of a digital delay generator. The value, S_t, received from the integration of the average voltage signal is a sum of two components: the integral from the average LIF signal of OH radicals, S_{OH}, which is proportional to the absolute OH concentration, and the integral from the average scattered light signal, S_{sc}. S_{sc} was directly measured in the absence of the hydroxyl radicals in the reactor.

We used four individually controlled flows of He (main carrier gas flow), H_2O/He, N_2O/He or HNO_3/He, and molecular substrate/Ar to prepare a reaction gas mixture. H_2O was transported to the reaction cell by bubbling a flow of He through water at controlled pressure and temperature in a thermostabilized saturator. HNO_3 was added to the third flow of He by bubbling this flow through 70% nitric acid aqueous solution in another thermostabilized saturator. (See ref 15 for details.) Molecular substrates (*n*- or *i*-C_3H_7Br) were accurately, manometrically diluted with argon by use of a Pyrex vacuum system. To minimize systematic error in molecular substrate concentration determination, we prepared four mixtures of *n*-C_3H_7Br in Ar and four mixtures of *i*-C_3H_7Br in Ar with different concentrations of molecular substrate, 2.45−5.07% and 3.26−6.53%, respectively. All flows were premixed in a delivery system and then directed through the reaction cell. The total flow rate ranged between 6.2 and 9.1 STP $cm^3\ s^{-1}$. The total pressure in the reactor was measured with 100.00 or 1000.0 Torr (1 Torr = 133.322 Pa) capacitance manometers. The reaction gas temperature in the detection zone was monitored with a retractable Chromel−alumel thermocouple. The maximum total uncertainty in the measurements of the reaction temperatures, *T*, did not exceed 0.5% of *T*.[14,15]

The molecular concentration of each reactant in the detection zone was calculated by means of multiplying the three values: the total concentration derived from the measured total pressure and temperature by use of the ideal gas law, the molecular partial concentration in the flow carrying the reactant, and the value from the ratio of the flow carrying the reactant to the total gas flow rate. Typical reaction mixtures used in the present experiments consisted of the following molecular concentration ranges, in units of molecule cm^{-3}: N_2O, $4.40 \times 10^{13}-1.17 \times 10^{15}$ or 0.0; HNO_3, 0.0 or $1.3 \times 10^{14}-7.5 \times 10^{14}$; H_2O, $8.6 \times 10^{14}-6.7 \times 10^{15}$; He, $6.76 \times 10^{17}-6.52 \times 10^{18}$; *n*-$C_3H_7Br$, $0.0-1.62 \times 10^{15}$ or 0.0; *i*-C_3H_7Br, 0.0 or $0.0-1.85 \times 10^{15}$; Ar, $0.0-2.65 \times 10^{16}$.

The chemicals utilized in this work had the following specified minimum purities (and suppliers): He, 99.999% (The BOC Group, Inc.); Ar, 99.999% (The BOC Group, Inc.); N_2O, 9.98% mixture of 99.99% purity in 99.999% He (The BOC Group, Inc.); H_2O, ACS reagent-grade (Sigma−Aldrich); HNO_3, 70% aqueous solution, ACS reagent-grade (Sigma−Aldrich); *n*-C_3H_7Br, 99.7% (Sigma−Aldrich); *i*-C_3H_7Br, 99.6% (Sigma−Aldrich). Both bromopropanes were purified by vacuum distillation prior to use. The chemical purities of these samples were examined by gas chromatography/mass spectrometry (GC/MS). After purification by vacuum distillation, the purity of the samples of both bromopropanes exceeded the specifications provided by Sigma−Aldrich. A discussion of impurities in *n*- and *i*-C_3H_7Br samples and their potential influence on the final experimental results is given at the end of the next subsection.

II.B. Reaction Rate Measurements and Data Processing. All experiments measuring the bimolecular rate coefficients for reactions 1 and 2 were performed under pseudo-first-order kinetics conditions with a large excess of molecular substrate concentration ([*n*-C_3H_7Br], [*i*-C_3H_7Br]) with respect to the initial concentration of the hydroxyl radical, $[OH]_0$, which ranged approximately from 6×10^9 to 3×10^{11} molecule cm^{-3} in the detection zone. The initial concentrations of OH radicals were estimated in ways similar to those described in ref 14, in which OH radicals were generated by the 193-nm pulsed laser photolysis of N_2O via processes 3 and 4, and in ref 18, where OH was formed by applying 248-nm laser photolysis dissociation of HNO_3. Accurate knowledge of the initial OH radical concentration is not needed to determine the bimolecular rate coefficients because of all experiments being ran under pseudo-

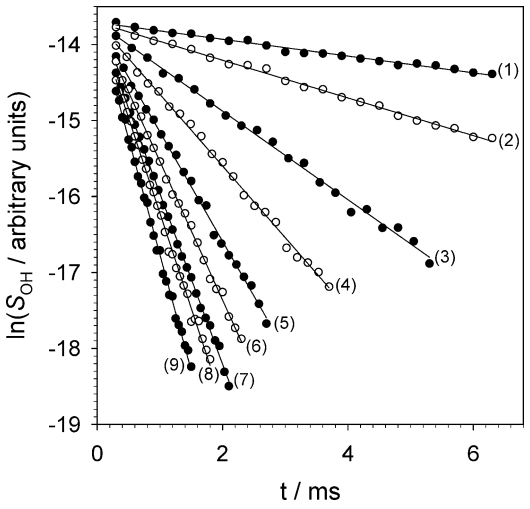

Figure 1. Examples of relative OH concentration temporal profiles obtained under the following experimental conditions: helium buffer gas, temperature $T = 720$ K, total pressure $P = 13.36$ kPa (100.2 Torr), $[N_2O] = 4.0 \times 10^{14}$ molecule cm^{-3}, $[H_2O] = 1.8 \times 10^{15}$ molecule cm^{-3}; [*n*-C_3H_7Br] = 0.0, 2.74×10^{13}, 7.84×10^{13}, 1.56×10^{14}, 2.52×10^{14}, 3.30×10^{14}, 4.04×10^{14}, 4.73×10^{14}, and 5.60×10^{14} molecule cm^{-3} for profiles 1−9, respectively.

first-order conditions with a large excess of molecular substrate. The estimated OH radical detection limit, defined by unity signal-to-noise ratio at 50 accumulated signals, was found to range from 1×10^8 to 3×10^8 molecule cm^{-3} depending on experimental conditions.

A typical set of relative OH concentration temporal profiles (a set of experiments) are shown in Figure 1 as a plot of ln (S_{OH}) = ln ($S_t - S_{sc}$) versus time delays, *t*. The initial detection time delay, t_0, was not less than 0.3 ms in all relative OH concentration decay profiles, which were subjected to data processing to obtain the reaction rate coefficients here. Molecules of water were always added to the reaction mixtures, at concentrations that were varied from 8.6×10^{14} to 6.7×10^{15} molecule cm^{-3} from set to set of experiments. This was done to ensure that the reaction of O(^{1}D) with H_2O, and/or rotational and vibrational equilibration of OH radicals to the Boltzmann distribution, proceeded sufficiently fast and had a negligible effect on the measured rate coefficients.[17,21] Furthermore, over the entire experimental temperature range, we selectively obtained temporal profiles of the formation of OH($X^2\Pi$, $v = 0$) under typical experimental conditions in the absence of molecular substrate. We observed a prompt OH($X^2\Pi$, $v = 0$) formation, which was always much faster than t_0, indicating that reaction 4 and/or the rotational and vibrational equilibration of OH radicals to the Boltzmann distribution proceeded fast enough to be neglected at the time delays $t \geq t_0$. Otherwise, a non-prompt OH($X^2\Pi$, $v = 0$) formation would have been observed due to the lack of completion of these processes.

Each set of experiments was analyzed, with the assumption of pseudo-first-order kinetics behavior of the hydroxyl radical decay, to determine bimolecular rate coefficients of the reactions:

$$\ln (S_{OH}) = \ln (S_t - S_{sc}) = \text{constant} - k't \qquad \text{(I)}$$

where the effective first-order rate coefficient, k', is given by

$$k' = k_i[MS] + k_0 \qquad \text{(II)}$$

k_i is the bimolecular rate coefficient of the reaction under study ($i = 1, 2$), [MS] is the molecular substrate concentration ([*n*-C_3H_7Br], [*i*-C_3H_7Br]), and k_0 is the effective first-order rate coefficient of the hydroxyl radical decay due to possible OH reactions with background impurities in the buffer gas, N_2O, H_2O, and HNO_3 precursors; OH reaction with HNO_3; and OH diffusion and flow out of the detection zone (OH background loss). The effective first-order rate coefficient values, k', were derived from linear least-squares fits of the experimental values ln (S_{OH}) to expression I. These least-squares fits and all next least-squares fits in the present work were performed with no weighting of the data points.

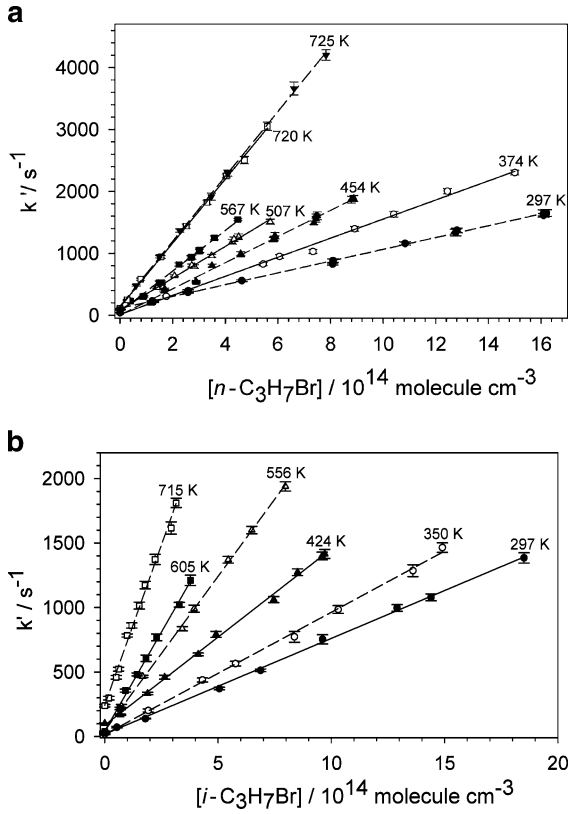

Figure 2. Examples of experimentally obtained (a) k' versus [*n*-C_3H_7Br] and (b) k' versus [*i*-C_3H_7Br] dependences.

Examples of effective first-order rate coefficient dependences on molecular substrate concentration are presented in Figure 2 for *n*- and *i*-C_3H_7Br substrates (panels a and b, respectively). We determined the bimolecular rate coefficient, k_i, from the slope of the least-squares straight line drown through the k' versus [MS] data points including the (0, k_0) point, where k_0 was derived from the OH temporal profile directly measured at zero concentration of the molecular substrate.

To evaluate quantitative effects of impurities in samples of *n*- and *i*-propyl bromide on the measured bimolecular rate coefficients, the samples of both bromopropanes were analyzed for contaminants. GC/MS (Agilent Technologies 6890N gas chromatography system/5973 mass selective detector) was used in these analyses. It was found that, after purification by vacuum distillation, the purity of both bromopropanes (*n*-C_3H_7Br, 99.81%; *i*-C_3H_7Br, 99.80%) exceeded the specifications provided by the supplier. The GC/MS analysis revealed the presence of the following impurity levels: *n*-C_3H_7OH (0.012%), *i*-C_3H_7Br (0.093%), (n-C_3H_7)$_2$O (0.080%), and *n*-C_4H_9Br (0.010%) in the *n*-propyl bromide sample and CH_2═$CHCH_3$ (0.006%), *i*-C_3H_7OH (0.061%), *n*-C_3H_7Br (0.045%), *n*-C_4H_9Br (0.018%), and $CH_3CHBrCH_2Br$ (0.071%) in the *i*-propyl bromide sample. In order to eliminate contributions from OH reactions with impurities to the final experimental results of

TABLE 1: Conditions and Results of Experiments on the Reaction of Hydroxyl Radicals with *n*-Propyl Bromide

no.[a]	*T*, K	*P*, kPa	[*n*-C_3H_7Br] range, 10^{14} molecule cm^{-3}	*I*,[b] mJ $pulse^{-1}$ cm^{-2}	$[OH]_0$, 10^{10} molecule cm^{-3}	k_1,[c] 10^{-13} $molecule^{-1}$ cm^3 s^{-1}
1*	297	13.36	1.23−16.2	4.3	4	9.36 ± 0.24
2*	297	6.69	1.41−16.2	14	6	9.60 ± 0.39
3*	297	6.69	1.40−16.1	14	6	9.56 ± 0.41
4*	341	26.73	1.35−13.2	12	2	12.06 ± 0.51
5*	341	26.73	1.32−13.4	12	2	12.24 ± 0.54
6	374	26.75	1.76−15.0	0.62	10	15.27 ± 0.80
7*	409	13.37	0.779−7.05	3.2	2	17.69 ± 0.74
8*	454	26.71	1.67−8.88	10	10	20.98 ± 0.77
9*	507	13.37	0.891−5.71	3.7	5	25.48 ± 0.83
10*	567	13.36	0.396−4.48	2.7	1	32.6 ± 1.3
11	650	13.37	0.299−3.60	2.1	4	40.9 ± 1.4
12	691	26.69	0.489−3.91	0.32	4	48.7 ± 2.4
13	720	13.36	0.276−5.59	2.0	30	50.9 ± 1.2
14	720	13.36	0.274−5.60	2.0	30	51.4 ± 1.3
15	725	26.66	0.669−4.8	0.46	2	52.1 ± 2.2
16	725	13.33	0.595−7.75	1.7	8	51.0 ± 1.6
17	725	13.33	0.605−7.83	1.7	8	52.2 ± 1.1

[a] Experiment number. OH was produced by the PLP of HNO_3 at 248 nm in experiments marked with asterisks; OH was formed by the 193-nm PLP of N_2O to $O(^1D)$ and N_2 and the subsequent rapid reaction of $O(^1D)$ with H_2O in unmarked experiments. [b] Photolysis laser intensity. [c] Error limits represent 2σ statistical uncertainties only. Maximum estimated systematic uncertainty is 5% of the bimolecular rate coefficient value (see refs 14 and 15 for details).

TABLE 2: Conditions and Results of Experiments on the Reaction of Hydroxyl Radicals with *i*-Propyl Bromide

no.[a]	*T*, K	*P*, kPa	[*i*-C_3H_7Br] range, 10^{14} molecule cm^{-3}	*I*,[b] mJ $pulse^{-1}$ cm^{-2}	$[OH]_0$, 10^{10} molecule cm^{-3}	k_2,[c] 10^{-13} $molecule^{-1}$ cm^3 s^{-1}
1	297	13.38	0.534−18.5	0.77	4	7.37 ± 0.19
2	297	26.72	0.552−14.4	0.23	6	7.51 ± 0.13
3	297	26.72	0.545−14.6	0.23	6	7.70 ± 0.21
4	350	26.74	1.92−14.9	0.28	6	9.44 ± 0.33
5	350	26.74	1.94−13.4	0.28	6	9.21 ± 0.41
6	409	13.40	0.480−6.10	0.65	0.6	12.13 ± 0.38
7*	424	13.42	0.694−9.71	2.3	4	13.63 ± 0.43
8*	453	13.35	1.01−8.51	4.8	3	14.97 ± 0.62
9	506	13.38	0.448−5.15	0.46	2	19.49 ± 1.1
10	506	13.38	0.447−5.16	0.46	2	19.69 ± 1.4
11	556	26.76	0.738−7.97	0.31	4	23.91 ± 0.53
12	605	13.39	0.660−3.79	1.4	10	29.6 ± 1.7
13	605	13.39	0.680−3.78	1.4	10	30.7 ± 1.5
14	665	26.66	0.456−4.32	0.25	8	39.3 ± 1.9
15	701	13.36	0.335−3.82	0.46	7	46.3 ± 2.8
16	715	13.41	0.278−2.95	1.2	10	47.7 ± 2.9
17	715	26.65	0.337−3.68	1.0	2	48.1 ± 2.6
18	715	6.67	0.503−3.15	0.31	7	49.6 ± 2.5

[a−c] Footnotes are as described for Table 1.

the bimolecular rate coefficients for reactions 1 and 2, we had to make corrections for OH disappearance via reactions with the detected impurity compounds in the *n*- and *i*-C_3H_7Br samples. For calculating these corrections, we applied the same procedure as described in earlier work[16] with previously published bimolecular rate coefficients[2,7,17,22−26] for OH reactions with corresponding impurity molecules. The resultant impurity corrections are −1.8% and −0.7% for the bimolecular rate coefficients of reactions 1 and 2, respectively, at the lowest temperature ($T = 297$ K), and their absolute values are smaller at higher temperatures of this study. The bimolecular rate coefficients for reactions 1 and 2 presented in Tables 1 and 2 are already impurity-corrected values.

II.C. Experimental Results. The kinetics study of the gas-phase OH radical reactions with *n*- and *i*-C_3H_7Br was performed over the temperature ranges of 297−725 and 297−715 K and at pressures of 6.69−26.75 and 6.67−26.76 kPa, respectively. The conditions and results of utilized experiments to determine the values of the bimolecular rate coefficients for reactions 1 and 2 are compiled in Tables 1 and 2.

The initial concentration of hydroxyl radicals was varied from set to set of experiments by changing the photolysis laser intensity or the concentration of N_2O or HNO_3 in wide ranges. The measured rate coefficients demonstrate no correlation with pressure and initial concentration of OH radicals within the experimental ranges. The observed pressure independence for both reactions was anticipated, since the mechanisms of reactions 1 and 2 are expected to be those of hydrogen-atom abstraction by hydroxyl radical. The fact that the rate coefficients are independent of the initial OH radical concentration indicates the absence of any influence from potential secondary reactions on the kinetics of OH radical decay that should be due to the low values of $[OH]_0$ in the detection zone ($[OH]_0 \approx (0.6-30) \times 10^{10}$ molecule cm^{-3}). There was no correlation between the measured rate coefficients and the photolysis laser intensity or wavelength within the experimental ranges. This fact allows one to consider the possible effects of the reaction between OH and the products of laser photolysis of *n*- or *i*-C_3H_7Br on the rate coefficient measurements as negligible in our experiments. At the highest temperatures in this study, the absence of any

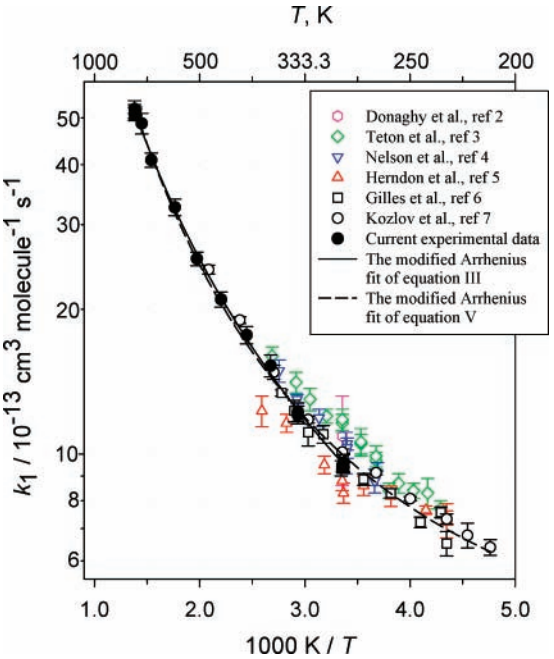

Figure 3. Temperature dependence of the bimolecular rate coefficient for the reaction of OH with *n*-C_3H_7Br displayed in Arrhenius coordinates.

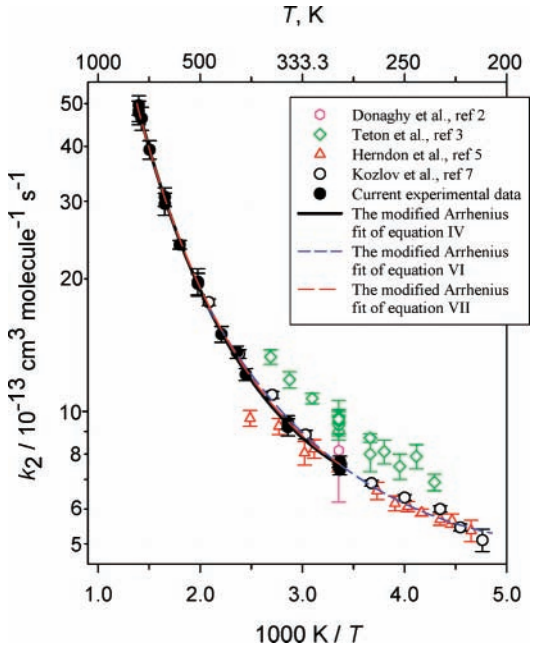

Figure 4. Temperature dependence of the bimolecular rate coefficient for the reaction of OH with *i*-C_3H_7Br displayed in Arrhenius coordinates.

potential influence from thermal decomposition of both bromopropanes on the final results was verified by measuring the bimolecular rate coefficients at different bulk flow velocities and reaction pressures that varied by factors of 2.6 and 2.0 for reaction 1 and by factors of 2.8 and 4.0 for reaction 2.

The bimolecular rate coefficients for reactions 1 and 2 determined in our study are plotted along with those from the previous studies[2−7] in Figures 3 and 4. The rate coefficient data sets for reactions 1 and 2 obtained in our experiments [$k_1(T)$ and $k_2(T)$ data sets] exhibit positive temperature dependencies with positive curvatures in the Arrhenius graphs. Three-parameter, nonlinear least-squares fits of these data sets to the modified Arrhenius expression yield the following optimized expressions for the bimolecular rate coefficient temperature dependencies of reactions 1 and 2 within their corresponding experimental temperature ranges:

$$k_1(T) = (1.32 \times 10^{-17})T^{1.95}\exp(+25/T)\ \text{cm}^3\ \text{molecule}^{-1}\ \text{s}^{-1} \quad (297-725\ \text{K})\quad \text{(III)}$$

$$k_2(T) = (1.56 \times 10^{-24})T^{4.18}\exp(+922/T)\ \text{cm}^3\ \text{molecule}^{-1}\ \text{s}^{-1} \quad (297-715\ \text{K})\quad \text{(IV)}$$

The maximum and the average square deviations of the experimental bimolecular rate coefficients from those calculated from the above parametrized expressions are only 4.0% and 1.8% for expression III and 3.4% and 1.7% for expression IV. Thus expressions III and IV reproduce our experimental data sets of the measured rate coefficients very well. Error limits of the parameters in expressions III and IV are not reported here, as these parameters bear no physical meaning.

To verify the absence of interference from molecular substrate (*n*- or *i*-C_3H_7Br) adsorption and desorption processes on the walls of the vacuum, delivery systems, and the reactor, we varied the following parameters: the surface-to-volume ratio of the Pyrex vessels for *n*-C_3H_7Br/Ar and *i*-C_3H_7Br/Ar mixture preparation and storage as well as the calibrated Pyrex vessels used to measure the flow rates (varied by a factor of 3 at least); the molecular substrate concentration of the *n*-C_3H_7Br/Ar and *i*-C_3H_7Br/Ar mixtures (see subsection II.A); bulk flow velocities in the delivery system and in the reactor (varied by factors of approximately 4 and 2, respectively); and pressure (see Tables 1 and 2). No correlation was found between those parameters and the measured bimolecular rate coefficients within the experimental ranges. Invariance of the bimolecular rate coefficients with respect to the experimental parameters described above gives us confidence in the bimolecular rate coefficients for reactions 1 and 2 measured in the present work.

III. Comparison with Previous Studies and Discussion

The kinetics studies of reactions 1 and 2 were performed in previous works[2−7] at low temperatures related to the chemistry of the Earth's atmosphere. The results of these studies cover the temperature range from 210 to 480 K. The present study provides the first direct experimental determination of the temperature dependences of the bimolecular rate coefficients of reactions 1 and 2 performed at high temperatures extended from 297 K (to compare with the earlier studies[2−7]) to 725 and 715 K, respectively, which is relevant to combustion and other thermal processes. Our measurements are in good agreement with the majority of earlier investigations conducted with different kinds of experimental approaches, such as relative reaction rate method coupled with the gas chromatograph analytical technique,[2] PLP/PLIF,[3,5,6] discharge flow/LIF,[4] and flash photolysis/resonance fluorescence techniques[7] (see Figures 3 and 4).

III.A. OH + *n*-C_3H_7Br Reaction. The results of the present experiments on reaction 1 agree nearly perfectly in common temperature ranges with the most extensive and recently obtained data sets for low temperatures from the publications by Gilles et al.[6] and Kozlov et al.[7] Indeed, if our $k_1(T)$ data set is combined with the $k_1(T)$ data sets reported in refs 6 and 7, then the nonlinear least-squares fit of the resultant combined $k_1(T)$ data set to the modified three-parameter Arrhenius

expression yields the bimolecular rate coefficient temperature dependence of reaction 1:

$$k_1(T) = (1.89 \times 10^{-19})T^{2.54}\exp(+301/T)\ \text{cm}^3\ \text{molecule}^{-1}\ \text{s}^{-1} \quad (210-725\ \text{K}) \quad \text{(V)}$$

The maximum and average square deviations of experimental bimolecular rate coefficient values of the resultant combined data set from those values calculated by use of expression V are only 6.9% and 3.8% of the calculated value, respectively, for the entire temperature range from 210 to 725 K.

The first study of the reactivity of OH with *n*-C_3H_7Br was executed by Donaghy et al.[2] using the relative reaction rate technique. They measured a ratio between the rate coefficients of reaction 1 and the reaction of the hydroxyl radical with cyclohexane at $T = 298$ K only. The product of the obtained ratio in ref 2 and the bimolecular rate coefficient for the reaction of the hydroxyl radical with cyclohexane evaluated by Atkinson[24] gives $k_1(298\ \text{K}) = (1.09 \pm 0.23) \times 10^{-12}$ cm^3 molecule^{-1} s^{-1}. This value agrees with the k_1 value given by expression V at $T = 298$ K within experimental error.

Téton et al.[3] performed the first direct investigation of the temperature-dependent kinetics of reaction 1 in the temperature range 233−372 K. As can be seen from Figure 3, the experimental $k_1(T)$ data reported by Téton et al.[3] are systematically higher than k_1 values calculated from expression V. The maximum and arithmetical average deviations are 18.1% and 11.6%, respectively. Nevertheless, the data from ref 3 are generally consistent with the combined $k_1(T)$ data sets of Gilles et al.[6] and Kozlov et al.[7] and the data set obtained in this work when compared with their experimental uncertainties. The results measured by Nelson et al.[4] are in good agreement with our results and those from refs 6 and 7.

The bimolecular rate coefficients measured by Herndon et al.[5] agree well with expression V in the temperature range 230−281 K, but they are systematically lower at higher temperatures used in ref 5 than those given by expression V (see Figure 3). The maximum of these deviations reaches 19.7% at the highest temperature $T = 386$ K of the experiments carried out by Herndon et al.[5] These rate coefficient data from ref 5 were probably superseded by those data for reaction 1 measured again in the same laboratory and published a few months later,[6] which are in excellent agreement with the present data and those from ref 7, as has already been pointed out. A probable reason for this disagreement between the data published by Herndon et al.[5] and those published by Gilles et al.[6] is discussed in subsection III.B.

III.B. OH + *i*-C_3H_7Br reaction. The bimolecular rate coefficients for reaction 2 measured in our experiments are in excellent agreement with the most extensive and recently obtained data published by Kozlov et al.[7] over a common temperature range. This $k_2(T)$ data set combines well with our $k_2(T)$ data set. The nonlinear least-squares fits of this resultant combined $k_2(T)$ data set to the modified three-parameter Arrhenius expression give the bimolecular rate coefficient temperature dependencies of reaction 2 within the corresponding temperature ranges:

$$k_2(T) = (2.83 \times 10^{-21})T^{3.1}\exp(+521/T)\ \text{cm}^3\ \text{molecule}^{-1}\ \text{s}^{-1} \quad (210-480\ \text{K}) \quad \text{(VI)}$$

$$k_2(T) = (4.54 \times 10^{-24})T^{4.03}\exp(+860/T)\ \text{cm}^3\ \text{molecule}^{-1}\ \text{s}^{-1} \quad (297-715\ \text{K}) \quad \text{(VII)}$$

The maximum and the average square deviations of the experimental rate coefficients from those given by above parametrized expressions are only 5.0% and 2.8% for expression VI and 5.0% and 2.2% for expression VII, respectively. The resultant combined $k_2(T)$ data set of our data and those of Kozlov et al.[7] exhibits significant positive curvature in the Arrhenius plot. Therefore, we have suggested two curves, VI and VII, for the low and high temperature ranges to reproduce experimental data more precisely.

As described in the Introduction, reaction 2 can proceed through two exothermic channels of H-atom abstraction by OH, from CH_3 or CHBr groups, so the observed significant positive curvature of the rate coefficient temperature dependence for this reaction in the Arrhenius coordinates is probably the result of temperature-dependent competition between these two reaction pathways. We cannot quantitatively judge the branching ratios of reactions 1 and 2 for formation of isomeric brominated propyl radicals, since we measured only OH decay and not products in the experiments.

Donaghy et al.[2] performed the first investigation of OH reactivity with *i*-C_3H_7Br using the relative reaction rate method. The rate coefficient of reaction 2 was measured with respect to reaction of the hydroxyl radical with cyclohexane at $T = 298$ K only. Multiplication of the ratio obtained in ref 2 and the bimolecular rate coefficient for OH reaction with cyclohexane evaluated by Atkinson[24] gives $k_2(298\ \text{K}) = (8.2 \pm 1.9) \times 10^{-13}$ cm^3 molecule^{-1} s^{-1}. This value agrees with those given by expressions VI and VII at $T = 298$ K.

Téton et al.[3] performed the first direct study of the temperature-dependent kinetics of reaction 2 in the temperature range 233−372 K. As can be seen from Figure 4, the experimental $k_2(T)$ data reported in ref 3 are systematically higher than k_2 values calculated from expression VI. The maximum, minimum, and arithmetical average deviations are 31.6%, 17.6%, and 23.8%, respectively, which are higher than the experimental uncertainties. So the data measured by Téton et al.[3] are not consistent with the combined $k_2(T)$ data sets of our data and that from ref 7 as compared with their experimental uncertainties.

The reaction 2 bimolecular rate coefficients of Herndon et al.[5] measured at temperatures from 215 to 402 K are in excellent agreement with values given by expression VI in the temperature range 215−321 K, but the rate coefficients obtained at three of the highest temperature measurements,[5] 331, 361, and 402 K, are systematically lower by 9.0%, 8.9%, and 21.2%, respectively, than those calculated from expression VI (see Figure 4).

This disagreement can be explained as follows. In the kinetics study of reactions 1 and 2 executed by Herndon et al.,[5] hydroxyl radicals were generated by the PLP of HONO molecules at 355 nm (see the Supporting Information for ref 5). Nitrous acid, HONO, was prepared by dropwise addition of 0.1 M sodium nitrite to 10% H_2SO_4 at 273 K.[5] According to the article published by Becker et al.,[27] NO_2 is also formed in gas phase as a byproduct of this synthesis. The NO_2 concentration can be significant if the reaction mixture is not frequently refreshed in the flask in which the synthesis was performed. Thus, NO_2 could be present in the reactor of PLP/PLIF apparatus during the experimentation by Herndon et al.[5] The PLP of NO_2 at 355 nm gives NO and O(^{3}P) as main products.[17] In this case, OH decay

can be affected by OH generated via the reaction of $O(^3P)$ with *n*- or *i*-C_3H_7Br. Such additional OH production would have had the effect of delaying OH decay and thus would have reduced the derived rate coefficients for reactions 1 and 2 in ref 5. It should be noted that the discussion presented here is purely speculative, as neither the rate coefficients of the $O(^3P)$ reactions with *n*- and *i*-C_3H_7Br nor the exact values of NO_2 molecule concentrations formed in the experiments by Herndon et al.[5] are known. The bimolecular rate coefficients of reaction 1 published by Gilles et al.[6] were not significantly affected by the potential presence of NO_2, because the reaction mixture used in HONO synthesis was refreshed daily (frequently).[6]

IV. Summary

We have measured the bimolecular rate coefficients for the reactions of OH radicals with *n*- and *i*-C_3H_7Br by using the PLP/PLIF technique to improve the kinetics data base for these two species. Our results confirm most of the previous low-temperature studies and extend the present kinetics knowledge of reactions 1 and 2 to high temperatures. We recommend expression V for the bimolecular rate coefficient temperature dependence of reaction 1 in the temperature range 210−725 K and expressions VI and VII for the bimolecular rate coefficient temperature dependences of reaction 2 in the temperature ranges 210−480 and 297−715 K, respectively, for the purpose of kinetic modeling.

Acknowledgment. This research was supported by the Patrick F. Taylor Chair Foundation. We thank Dr. J. N. Crowley, Dr. V. D. Knyazev, Dr. V. L. Orkin, and Mr. W. M. Gehling, Jr. for helpful discussion and advice.

References and Notes

(1) United Nations Environment Programme. *Report of the 26th meeting of the Open-ended Working Group of the Parties to the Montreal Protocol*, Montreal, 3−6 July 2006.

(2) Donaghy, T.; Shanahan, I.; Hande, M.; Fitzpatrick, S. *Int. J. Chem. Kinet.* **1993**, *25*, 273.

(3) Téton, S.; El Boudali, A.; Mellouki, A. *J. Chim. Phys.* **1996**, *93*, 274.

(4) Nelson, D. D., Jr.; Wormhoudt, J. C.; Zahniser, M. S.; Kolb, C. E.; Ko, M. K. W.; Weisenstein, D. K. *J. Phys. Chem. A* **1997**, *101*, 4987.

(5) Herndon, S. C.; Gierczak, T.; Talukdar, R. K.; Ravishankara, A. R. *Phys. Chem. Chem. Phys.* **2001**, *3*, 4529.

(6) Gilles, M. K.; Burkholder, J. B.; Gierczak, T.; Marshall, P.; Ravishankara, A. R. *J. Phys. Chem. A* **2002**, *106*, 5358.

(7) Kozlov, S. N.; Orkin, V. L.; Huie, R. E.; Kurylo, M. J. *J. Phys. Chem. A* **2003**, *107*, 1333.

(8) Espinosa-García, J. *Chem. Phys. Lett.* **2003**, *377*, 607.

(9) Rangel, C.; Navarrete, M.; Corchado, J. C.; Espinosa-García, J. *J. Mol. Struct. (THEOCHEM)* **2004**, *679*, 207.

(10) Chase, M. W., Jr. *J. Phys. Chem. Ref. Data* **1998**, *Monogr. 9*, 1−1951.

(11) Pedley, J. B.; Naylor, R. D.; Kirby, S. P. *Thermochemical Data of Organic Compounds*, 2nd ed.; Chapman and Hall: London, 1986.

(12) Orlando, J. J.; Tyndall, G. S. *J. Phys. Chem.* **1996**, *100* (50), 19398.

(13) Bodi, A.; Kercher, J. P.; Bond, C.; Meteesatien, P.; Sztáray, B.; Baer, T. *J. Phys. Chem. A* **2006**, *110*, 13425.

(14) Bryukov, M. G.; Knyazev, V. D.; Lomnicki, S. M.; McFerrin, C. A.; Dellinger, B. *J. Phys. Chem. A* **2004**, *108*, 10464.

(15) Bryukov, M. G.; Dellinger, B.; Knyazev, V. D. *J. Phys. Chem. A* **2006**, *110*, 936.

(16) Droege, A. T.; Tully, F. P. *J. Phys. Chem.* **1986**, *90*, 1949.

(17) Sander, S. P.; Friedl, R. R.; Golden, D. M.; Kurylo, M. J.; Moortgat, G. K.; Keller-Rudek, H.; Wine, P. H.; Ravishankara, A. R.; Kolb, C. E.; Molina, M. J.; Finlayson-Pitts, B. J.; Huie, R. E.; Orkin, V. L. *Chemical Kinetics and Photochemical Data for Use in Atmospheric Studies, Evaluation No. 15*; −Jet Propulsion Laboratory Publication 06-2; California Institute of Technology: Pasadena, CA, 2006.

(18) Gilles, M. K.; Burkholder, J. B.; Ravishankara, A. R. *Int. J. Chem. Kinet.* **1999**, *31*, 417.

(19) Wollenhaupt, M.; Carl, S. A.; Horowitz, A.; Crowley, J. N. *J. Phys. Chem. A* **2000**, *104*, 2695.

(20) D'Ottone, L.; Campuzano-Jost, P.; Bauer, D.; Hynes, A. J. *J. Phys. Chem. A* **2001**, *105*, 10538.

(21) Silvente, E.; Richter, R. C.; Hynes, A. J. *J. Chem. Soc., Faraday Trans.* **1997**, *93*, 2821.

(22) Yujing, M.; Mellouki, A. *Chem. Phys. Lett.* **2001**, *333*, 63.

(23) Mellouki, A.; Téton, S.; Le Bras, G. *Int. J. Chem. Kinet.* **1995**, *27*, 791.

(24) Atkinson, R. *Atmos. Chem. Phys.* **2003**, *3*, 2233.

(25) Spangenberg, T.; Köhler, S.; Hansmann, B.; Wachsmuth, U.; Abel, B.; Smith, M. A. *J. Phys. Chem. A* **2004**, *108*, 7527.

(26) Yujing, M.; Mellouki, A. *Phys. Chem. Chem. Phys.* **2001**, *3*, 2614.

(27) Becker, K. H.; Kleffmann, J.; Kurtenbach, R.; Wiesen, P. *J. Phys. Chem.* **1996**, *100*, 14984.